Preparation of uncurled and planar multilayered graphene using polythiophene derivatives via liquid-phase exfoliation of graphite

Hiroki Iguchi,[1] Koki Miyahara,[1] Chisato Higashi,[1] Keisuke Fujita,[1] Naoki Nakagawa,[1] Shunsuke Tamba,[1] Atsunori Mori,[1] Hiroshi Yoshitani,[2] Akira Nakasuga,[2] and Tatsuo Maruyama[1,*]

[1]Department of Chemical Science and Engineering, Graduate School of Engineering, Kobe University, 1-1 Rokkodaicho, Nada-ku, Kobe 657-8501, Japan

[2]Sekisui Chemical Co., Ltd., 2-1 Hyakuyama, Shimamoto-cho, Mishima-gun, Osaka 618-0021, Japan

Corresponding Author

*E-mail: tmarutcm@crystal.kobe-u.ac.jp

Short Title: Preparation of graphene using polythiophene

Keywords: in-situ morphology; graphene nanosheets; polythiophene; wrinkleless

ABSTRACT

We have investigated the effects of the preparation conditions of polythiophene/graphene complexes on their dispersion in organic solvents, and on the in-solution morphology of the multilayered graphene. Among four different regioregular polythiophene derivatives synthesized, poly(3-hexylthiophene) (P3HT) with a low molecular weight (*M*n 6000) was the most effective derivative for exfoliating graphite and for dispersing the multilayered graphene in toluene. Spectroscopic analysis revealed that P3HT interacted strongly with graphene to form a P3HT/graphene complex. We investigated the in situ morphology of multilayered graphene in organic solvents, using a flow particle image analyzer (FPIA) and revealed that the presence of polythiophenes produced larger P3HT/graphene complexes than that prepared in *N*-methylpyrrolidone (NMP). Microscopy analysis demonstrated that graphite flakes and multilayered graphene shrunk in the absence of P3HT when drying in organic solvents. The

presence of P3HT immobilized the extended morphology of the multilayered graphene by forming the complex. This prevented shrinkage of the multilayered graphene when drying in toluene. Transmission electron, atomic force and field-emission scanning electron microscopy observations revealed that the P3HT/graphene complex consisted of relatively flat and ultrathin multilayered graphene of approximately <10 nm in thickness. The polythiophene/graphene complexes had high electrical conductivity, which depended on the kinds of polythiophenes. These findings further our understanding of the morphology of multilayered graphene, and will promote the development of uncurled multilayered graphene.

1. Introduction

Graphene has attracted broad attention and is a promising nanomaterial, because of its useful properties including high electrical conductivity, high mechanical toughness, high gas-barrier performance, and optical properties [1-3]. Industrial applications of graphene are anticipated in areas including electronics, automotives, packaging, and medical engineering. In particular, the application of graphene in electronics has been widely studied. Geim *et al* first reported the preparation of graphene in 2004 [1]. There have since been many reported methods for preparing graphene and graphene nanosheets, including mechanical exfoliation [1], chemical vapor deposition (CVD) [4, 5], heat decomposition [6], and chemical syntheses [7, 8]. Many of these methods are costly, ineffective, and poorly scalable. The ‘liquid-phase exfoliation’ of graphite is one of the most inexpensive and scalable approaches [9-14]. However, the strong hydrophobic interactions and van der Waals forces between graphene sheets induces graphene to aggregate in solvents. This results in loss of the functional properties of graphene and makes it difficult to manipulate graphene in industrial situations. Liquid-phase exfoliation can be divided into covalent and non-covalent approaches. The covalent functionalization of graphene (e.g. graphene oxide, acidified graphene, and reduced graphene oxide) involves structural defects, and the resulting materials often exhibit a loss of properties [7, 15]. Thus,

recent studies have favored non-covalent approaches. Various substances (e.g. solvents, supramolecules, surfactants, polymers, ionic liquids, proteins, and nanotubes) have been proposed for use in the direct production of pristine graphene from graphite using non-covalent intermolecular interactions [11, 14, 16-25]. Many of these dispersants cover graphene surfaces with nonconductive molecules and decrease the electrical conductivity of graphene [24, 26].

Another challenge to be addressed is ensuring a satisfactory morphology of graphene in a solution phase. Since graphene is a two-dimensional ultrathin material, its morphology in solution is likely to affect its functional properties in applications [27]. For instance, the wrinkling, curling and folding of graphene alter its effective surface area, and affect its conductivity and reactivity. Zhang et al. reported that wrinkles in graphene promoted corrosion of a Cu surface [28]. Several papers have reported the wrinkling and curling of graphene nanosheets [27-34]. To the best of our knowledge, there are no reports on the in-solution morphology of graphene produced in a solution phase.

Polythiophenes (PTs) are π-conjugated polymers which show electrical conductivity, photoluminescence and good processability [35]. PTs can potentially exhibit π-π interactions with carbon nanomaterials such as carbon nanotubes, graphene and graphene oxides [36-41]. To overcome the loss of electrical conductivity of dispersant/graphene complexes, π-conjugated polymers can be used as conductive dispersants for graphene [39-43]. This can eliminate the process of dispersant decomposition, so highly conductive patterns can be obtained. We previously reported the exfoliation of pristine graphite in toluene using well-defined P3HT as a conductive dispersant. The resulting pristine multilayered graphene were prepared without loss of electrical conductivity, and showed high gas-barrier properties [44]. The molecular structure of the PT may affect the liquid-phase exfoliation of graphite flakes and the dispersion of multilayered graphene in solvents. This is supported by reports that the structures and molecular weights of PTs play a critical role in the dispersion of single-walled carbon nanotubes in toluene [45].

In the current study, we investigated the effects of the preparation conditions of PT/graphene

complexes on the dispersion of graphene and on the morphology of PT/graphene complexes. Spectroscopy analysis revealed that among the four different PTs that were investigated, P3HT exfoliated graphite flakes and produced stable graphene dispersions in toluene most effectively. Microscopy observations confirmed the production of ultrathin P3HT/graphene complexes, and indicated that P3HT immobilized the extended morphology of multilayered graphene both in solution and in dry conditions.

2. Materials and methods

2.1. Materials.

Graphite flakes were provided by Sekisui Chemical Co., Ltd. (Tokyo, Japan). Other chemicals were purchased from Wako Pure Chemical Industries, Ltd. (Osaka, Japan). Water used was deionized (Milli-Q, >15 MΩ cm^{-1}) using a Milli-Q Advantage A100 system equipped with an Elix UV 3 system (Millipore, Molsheim, France).

2.2. Preparation of polythiophenes derivatives (PTs).

PTs were synthesized using a slight modification of our previously reported procedure [46-49]. P3HT, P3HOT, P3OT, and P3SiT (Fig. 1a and Table S1) were synthesized by C-H functionalization polycondensation using a nickel catalyst.

2.3. Preparation of graphene dispersions.

“with pre-US”: Typically, toluene (10 g) containing graphite flakes (1 mg) was ultrasonicated using an Ultrasonic Cleaner VS-D100, 31 kHz (AsOne Corp., Osaka, Japan) at 25 °C for 1 h, after which it was mixed with toluene (3 g) containing PT (1 mg). The resulting mixture was ultrasonicated at 25 °C for 1 or 3 h, followed by a 10-fold dilution with toluene and a further 1 h of ultrasonication. Graphite flakes in toluene, multilayered graphene in *N*-methylpyrrolidone (NMP), and PT/graphene dispersions were prepared by this procedure. The concentrations of PT and graphite flakes were 6.6 μg/ml unless otherwise stated.

“w/o pre-US”: Graphite flakes (1 mg) were added to toluene (13 g) containing PT (1 mg). The resulting mixture was ultrasonicated at 25 °C for 2 or 4 h, followed by a 10-fold dilution with toluene and a further 1 h of ultrasonication.

2.4. Washing procedure to remove excess PT.

A PT/graphene dispersion (5.0 ml) containing 6.6 μg/ml of graphene were centrifuged at 10000 × g for 10 min to precipitate the PT/graphene complex. The supernatant (4.0 ml) was carefully removed, and fresh toluene (4.0 ml) was added. The dispersion was then ultrasonicated for 5 min. This procedure was repeated three times.

2.5. Characterization.

UV-Vis absorption spectra of dispersions (200–900 nm) were recorded using a V-770 double-beam spectrophotometer (JASCO, Hachioji, Japan). The PTs used in the present study do not absorb around 660 nm, so absorbance measurements at 660 nm allowed us to evaluate the concentration of graphene dispersed in the toluene. Fluorescence spectra were recorded using a FP-8200 fluorescence spectrophotometer (JASCO, Germany).

The number, equivalent circle diameter, and roundness of graphene sheets in the graphene dispersions were measured using a flow particle image analyzer (FPIA) (FPIA-3000S, Malvern Instruments, Malvern, Worcestershire, UK). Toluene and NMP were used as eluents for samples in toluene and in NMP, respectively. Samples (3.0 ml) containing PT/graphene complexes (6.6 μg/ml of graphene) were used for FPIA measurements.

TEM images were obtained using a JEOL 2100F transmission electron microscope operated at 200 kV (JEOL, Akishima, Japan). A droplet of PT/graphene dispersion was placed on a copper grid covered with elastic carbon film manufactured by Okenshoji Co., Ltd. (Tokyo, Japan), and then dried under vacuum at ambient temperature.

AFM images were obtained in tapping mode using a Nanonavi E-sweep microscope (Hitachi, Tokyo, Japan) with cantilevers at 17.0 N/m. A droplet of PT/graphene dispersion was placed on a p-Type

silicon wafer (Electronics and Materials Co., Ltd, Ashiya, Japan), and then dried under vacuum at ambient temperature.

Fluorescence microscopy images were obtained using an IX-71 inverted optical microscope (Olympus, Tokyo, Japan) with a fluorescence filter (WIB, excitation wavelength: 460–495 nm). The shrinkage of graphene during drying was observed using a VHX-6500 digital optical microscope (Keyence Corporation, Osaka, Japan). Drying was carried out by heating a glass slide containing a droplet of sample using a dryer.

Field-emission scanning electron microscope (FE-SEM) observations were carried out using a field-emission scanning electron microscope (JSM-7500F, JEOL, Tokyo, Japan) operating at an accelerating voltage of 7 kV. After silicon wafers were baked at 800 °C for 3 h in air, PT/graphene complex solutions were dropped on the wafers and dried under vacuum, followed by FE-SEM observations.

PT/graphene composites for the electric resistance measurements were prepared by suction filtration. A dry PT/graphene complex was re-dispersed in toluene by 20 min ultrasonication to give a graphene concentration of 0.33 gm/ml. The graphene concentration was determined based on the results of elemental analysis (Table S2). A PT/graphene dispersion was filtrated through filter paper that were 8 mm in diameter and 4 μm of pore size (Kiriyama Grass Co., Ltd.). PT/graphene on the filter paper was dried at 100 °C for 20 min and then vacuum-dried for 1 h to ensure complete solvent evaporation. Electrical resistance measurements were carried out using a four-point-probe ohmmeter (Mitsubishi Chemical Analytec Co., Ltd. LorestaAX MCP-T370, TFP-prove) for PT/graphene composites on filter paper. The data were collected at 4 different positions for each PT/graphene composite and averaged. Error bars represent standard deviations.

XRD patterns were recorded with a RINT2000 X-ray diffractometer (Rigaku, Akishima, Japan).

Thermogravimetric analysis was performed in an air atmosphere with a heating rate of 10 °C/min at Pt crucibles, using a Thermal analysis apparatus (Rigaku, Thermoplus EVO 2 TG8121, Japan).

X-ray photoelectron spectroscopy (XPS) spectra were recorded using a PHI X-tool X-ray photon

spectroscopic instrument (ULVAC, Chigasaki, Japan).

3. Results and discussion

3.1. Liquid-phase exfoliation of graphite flakes using polythiophenes.

Regioregular PTs were synthesized according to our previous reports (Fig. 1a) [46-49], and were used for preparing PT/graphene dispersions. To study the effect of the side chain structure of PT, four different kinds of PTs with controlled molecular weights were synthesized, which had *n*-hexyl, hexyl(oxymethyl), *n*-octyl and siloxane moieties as side chains. Two types of P3HTs with different molecular weights (*M*n) (6000 and 20000), which were termed P3HT6000 and P3HT20000, were also synthesized. Table S1 summarizes the molecular weights and regioregularities of the PTs. Graphite flakes were typically ultrasonicated at 25 °C for 1 h in toluene, and were then mixed with toluene solutions containing the PTs. They were then ultrasonicated at 25 °C for 2 or 4 h. Fig. 1b shows digital photos of graphite flakes in toluene and PT/graphene dispersions in toluene. Naked-eye observation suggested that graphene was not dispersed in toluene in the absence of a PT. The presence of the PT appeared to promote the dispersion of graphene in toluene. The various colors of the solutions were derived from the individual PTs (Fig. S1).

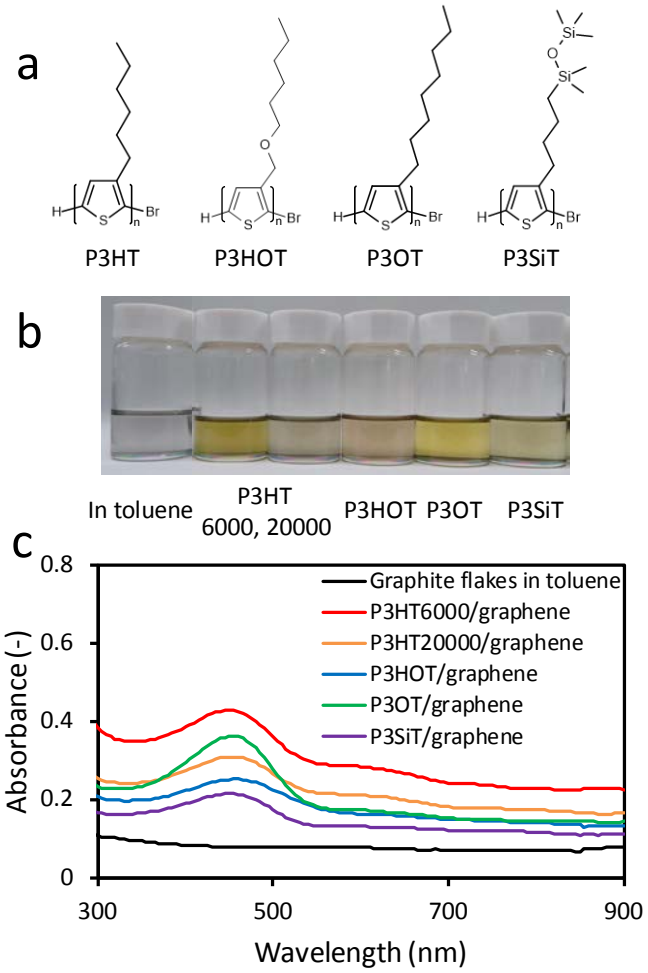

Fig. 1. (a) Chemical structures of polythiophenes (PTs) with different side chains. (b) Digital photos of graphite flakes in toluene and of PT/graphene dispersions in toluene. (c) Absorption spectra of graphite flakes in toluene and of PT/graphene dispersions in toluene. The concentrations of graphite flakes and PTs were 6.6 μg/ml. Graphite flakes were ultrasonicated for 1 h and were then added to solutions of the PTs, and the resulting suspensions ultrasonicated for 4 h.

To evaluate the effects of the PTs on graphene dispersion, we characterized PT/graphene dispersions by ultraviolet-visible (UV-Vis) absorption spectroscopy. Fig. 1c shows absorption spectra of the PT/graphene dispersions. The concentrations of the PTs and graphite flakes were 6.6 μg/ml for all cases. Graphene exhibited broad absorption at wavelengths higher than 300 nm (Fig. 1c, black line) [50-52]. The PTs exhibited strong absorption at around 450 nm (Fig. S1). Fig. 1c reveals that

P3HT6000 was the most effective for dispersing graphene among the PTs tested, which agreed with our previous reports [44]. P3HT with a low molecular weight (*M*n 6000) was considered to be effectively inserted between the graphene sheets to exfoliate graphite and multipoint interactions between P3HT and graphene stabilized the dispersion of graphene in solution. Bulky and flexible side-chains of the PTs (e.g. those of P3HOT and P3SiT) would distort the PT backbone due to steric hindrance. This backbone distortion would inhibit the adsorption of the PTs on graphene, and result in a lower dispersibility of graphene. These results and the results reported by Meng *et al.* [53] indicated that π–π interaction between a π-conjugated backbone of a PT and the graphene played an important role in the formation of the P3HT/graphene complex.

The high absorbances at 450 nm in the spectra in Fig. 1c were derived from the PTs in the PT/graphene complexes. Increasing the concentration of graphite flakes caused the relative absorbance at 450 nm (A_{450}–A_{550}) to decrease, while the absorption above 600 nm increased (Fig. S2a and b). These results suggested that the intrinsic absorbance of P3HT6000 at around 450 nm was affected by the interaction between P3HT and graphene, indicating a change in the electronic state of the π-conjugated system of P3HT. This was probably due to charge transfer or energy transfer from P3HT to the graphene, and/or π–π interaction between P3HT and the graphene [53].

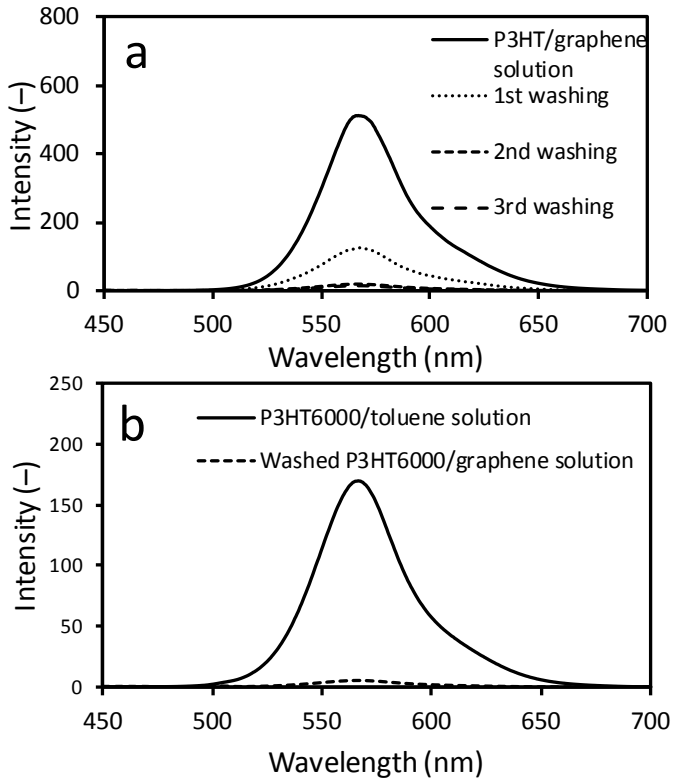

Fig. 2. (a) Fluorescence spectra of a P3HT6000/graphene dispersion before and after washing. (b) Quenching of P3HT6000 fluorescence induced by graphene. Fluorescence measurements were carried out at 25 °C. Excitation wavelength was 440 nm. The P3HT and graphene concentrations were 1 μg/ml and 4.33 μg/ml, respectively.

In a previous study, we prepared a P3HT/graphene complex which contained free P3HT (i.e. P3HT not adsorbed to graphene) [44]. To characterize this P3HT/graphene complex, we removed excess P3HT6000 from the P3HT6000/graphene complex by washing with excess toluene. Fig. 2a shows fluorescence spectra of the P3HT6000/graphene complex in toluene. As the washing process was repeated, the fluorescence of the P3HT6000/graphene complex decreased, indicating the removal of free P3HT6000. Elemental analysis of the washed P3HT6000/graphene complex indicated 3.6 wt.% of sulfur (Table S2), and thus that the P3HT6000 weight ratio in the complex was 0.19. Despite the significant decrease in fluorescence after washing, the P3HT6000/graphene complex still exhibited weak fluorescence. Fig. 2b shows fluorescence spectra of a P3HT6000 solution and the washed

P3HT6000/graphene dispersion, in which the P3HT concentrations were set at 1 μg/ml. The fluorescence intensity of the washed P3HT/graphene dispersion was 1/34 of that of the P3HT6000 solution. This indicated that graphene quenched the fluorescence of P3HT.

After washing the P3HT6000/graphene complex three times, the UV-Vis absorption spectrum of the complex in solution was measured. Fig. S3 shows that there was no obvious absorption around 450 nm, and that a broad weak absorption was observed at around 600 nm, which would have resulted from the formation of the P3HT/graphene complex. These fluorescence and absorption results revealed that P3HT directly interacted with the multilayered graphene and suggested the π-π interaction between P3HT and the graphene. This would contribute to the exfoliation of the graphite flakes and also to the stability of the multilayered graphene dispersion in toluene.

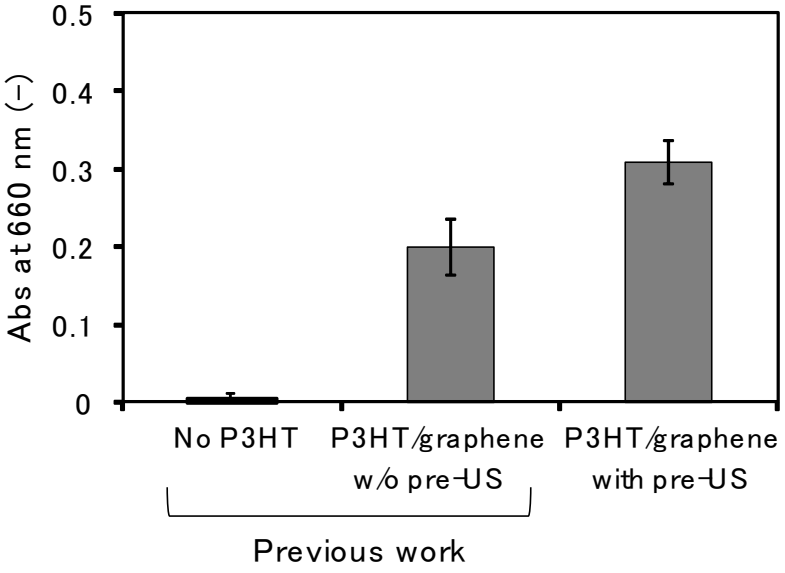

Fig. 3. Effect of preparation procedure for the P3HT/graphene dispersion on the absorbance at 660 nm. "w/o pre-US" indicates the procedure in which graphite flakes were added to the P3HT solution, followed by ultrasonication for 30 min. "with pre-US" indicates the procedure in which graphite flakes were ultrasonicated for 15 min, then added to the PT solution, followed by ultrasonication for another 15 min. The final concentrations of graphite flakes and P3HT were 0.33 mg/ml. The dispersions were

centrifuged at 1000×g for 20 min to remove unexfoliated particles and thick graphite flakes. The absorbance of the supernatant was then measured at 660 nm by UV-Vis absorption spectroscopy.

We then investigated the preparation procedure of the PT/graphene dispersion. In our previous study, graphite flakes were added to toluene solutions containing PTs which were then ultrasonicated, which is referred to as “w/o pre-US”. In the current study, graphite flakes were first ultrasonicated in toluene (i.e. ultrasonication pretreatment), after which they were added to PT solutions, followed by ultrasonication again, which is referred to as “with pre-US”. Fig. 3 shows that “with pre-US” was more effective for dispersing graphene than our previous procedure, “w/o pre-US”. The concentration of graphene obtained was 22 μg/ml, which was 1.5 times that obtained in our previous study. In the case of “w/o pre-US”, graphite flakes would be partly wrapped by P3HT, and some multilayered graphene would be interconnected with P3HT prior to exfoliation by ultrasonication. This presumably stabilized the graphite and nanosheet-stacked structure and inhibited exfoliation. The “with pre-US” procedure would produce pre-exfoliated multilayered graphene prior to P3HT addition, which would aid the insertion of P3HT between nanosheets. This would improve the dispersibility of exfoliated graphene with P3HT in toluene. These results implied that ultrasonication in toluene without any additives swelled the graphite flakes to some extent, and that the presence of a dispersant (i.e. PTs) stabilized the exfoliated state of graphene nanosheets in solution.

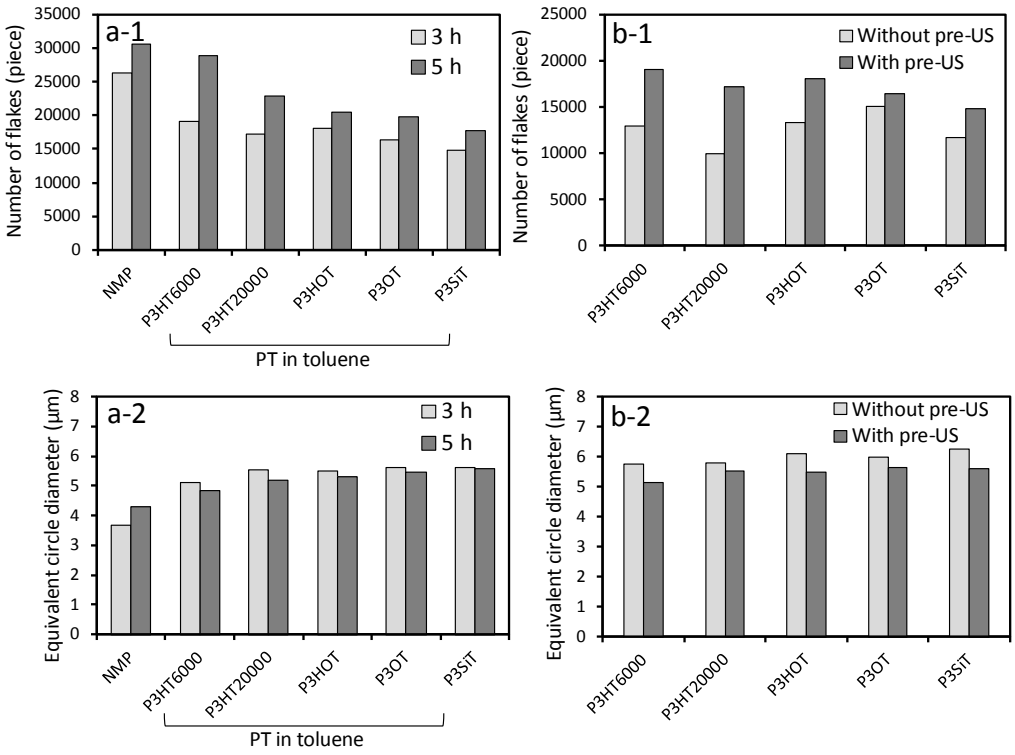

Fig. 4. FPIA analysis of PT/graphene dispersions. (a-1) Number and (a-2) equivalent circle diameter of multilayered graphene in NMP and PT/graphene complexes. PT/graphene dispersions were prepared by the "with pre-US" procedure. The concentrations of graphite flakes and PTs were both 6.6 μg/ml. The amount of sample solution was 3.0 ml. (b-1) Number and (b-2) equivalent circle diameter of multilayered graphene in PT/graphene complexes prepared by the "w/o pre-US" and "with pre-US" procedures. The sum of the ultrasonication times was 3 h. The concentrations of graphite flakes and PTs were both 6.6 μg/ml. The amount of sample solution was 3.0 ml.

3.2. Microscopy observations of washed PT/graphene complex.

The in-solution morphology of a two-dimensional layered material is of great importance for its functional properties in the liquid phase [34]. We evaluated the in-solution morphologies of the PT/graphene complexes in organic solvents by analyzing microscopy images in solution flow. A flow particle image analyzer (FPIA) can provide numerous microscopy images of microparticles in solution flow and statistical information on their size and shape in solution (Fig. S4a and b) [54]. NMP is

reportedly a good solvent for dispersing graphene [16, 20], so we used NMP as a control solvent in the FPIA measurements. The vertical axes of Fig. 4a-1 and a-2 represent the number of flakes (particles) and the average equivalent-circle diameter, respectively. Fig. 4a-1 shows that a relatively large number of multilayered graphene were dispersed in NMP simply by ultrasonication, and that ultrasonication for a longer duration (5 h) increased this number by 20%. Ultrasonication for 3 h in the presence of PTs also produced multilayered graphene, but less than that produced in NMP. There were negligible differences in the number of multilayered graphene produced in the presence of the different PTs during 3 h of ultrasonication. Ultrasonication for 5 h increased the number of multilayered graphene in the presence of all PTs. Ultrasonication for 5 h with P3HT6000 produced as many multilayered graphene as that in NMP. Among the PTs tested, P3HT6000 produced the largest number of multilayered graphene. This was consistent with the spectroscopy results in Fig. 1c. Fig. 4a-2 shows the average diameters of the multilayered graphene. Ultrasonication in NMP for 3 h produced small multilayered graphene (average diameter of less than 3.7 μm), while ultrasonication in the presence of PTs for 3 h produced multilayered graphene larger than 5 μm. These results indicated that the multilayered graphene shrunk or were somehow folded in NMP, while those containing P3HT were more expanded or unfolded in toluene. Ultrasonication for a longer duration (5 h) did not affect the diameter of the multilayered graphene.

Fig. 4b-1 and b-2 respectively show the number and diameter of multilayered graphene prepared by the “w/o pre-US” and “with pre-US” procedures. As shown in Fig. 3, the “with pre-US” procedure produced larger numbers of multilayered graphene for all PTs tested than the “w/o pre-US” procedure. The equivalent circle diameters were slightly smaller for “with pre-US” than for “w/o pre-US”.

Micrometer-sized multilayered graphene can be observed using an optical microscope. We observed the P3HT6000/graphene complex in this manner. The left column of Fig. S5a shows thick and large aggregates, indicating that graphite flakes dispersed in toluene without a PT were not exfoliated. Multilayered graphene prepared with P3HT6000 were observed under the microscope

before and after washing (Fig. S5b and c, respectively). Many of these multilayered graphene were 2–10 μm in diameter, which was consistent with the FPIA results. Fluorescent microscopy images (right column in Fig. S5) showed no detectable fluorescence in graphite flakes dispersed in toluene (Fig. 4a-1) and in washed multilayered graphene with P3HT6000 (Fig. S5c). The right column of Fig. S5b shows the yellow-green fluorescence derived from P3HT6000. These results also suggested that excess P3HT6000 in the toluene before washing (Fig. S5b) was sufficiently removed by the washing procedure (Fig. S5c).

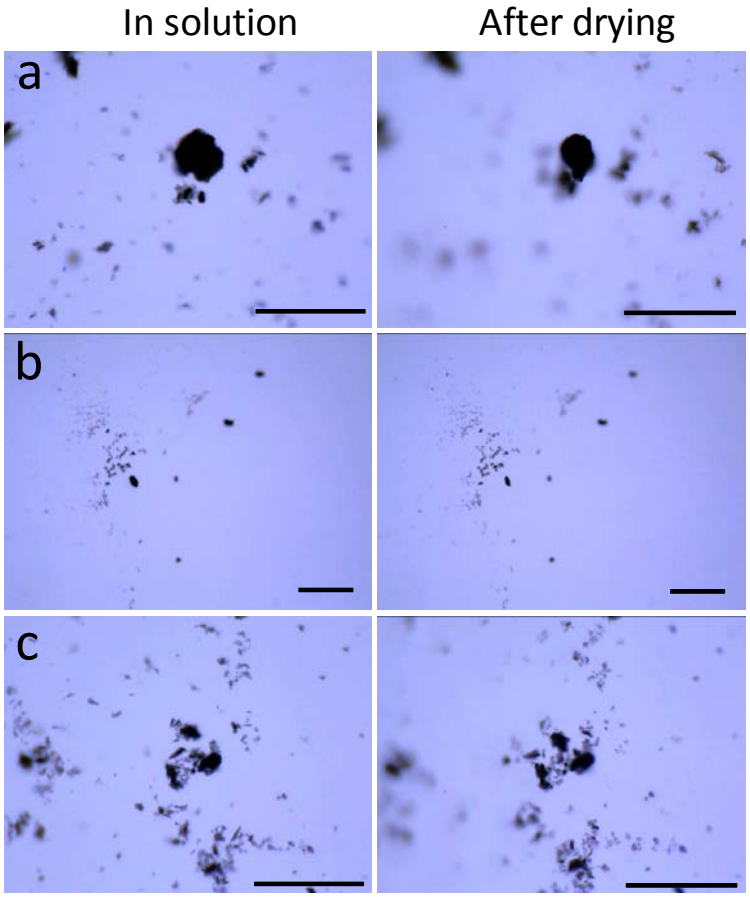

Fig. 5. Optical microscopy observations of graphite flakes and multilayered graphene in solution and in dry conditions. (a) Graphite flakes in toluene, (b) multilayered graphene in NMP, and (c) P3HT6000/graphene in toluene.

Graphene prepared by liquid-phase exfoliation for microscopy observations and practical applications frequently involves some form of drying process. We monitored the change in

morphology of multilayered graphene during drying. Fig. 5 shows optical microscopy images of graphite flakes and multilayered graphene in solution and after drying. Large aggregates of graphite flakes dispersed in toluene shrunk after drying (Fig. 5a), and multilayered graphene dispersed in NMP also shrunk after drying (Fig. 5b). Movies S1 and S2 (supplementary data) demonstrate the shrinkage of graphite flakes (in toluene) and multilayered graphene (in NMP) during drying, respectively. The morphology of the P3HT6000/graphene complex changed negligibly after drying, as shown in both Fig. 5c and Movie S1. These results indicated that the multilayered graphene shrunk during drying, and that P3HT6000 immobilized the extended morphology of the multilayered graphene by forming the complex. This led to negligible shrinkage of the P3HT6000/graphene complex during drying.

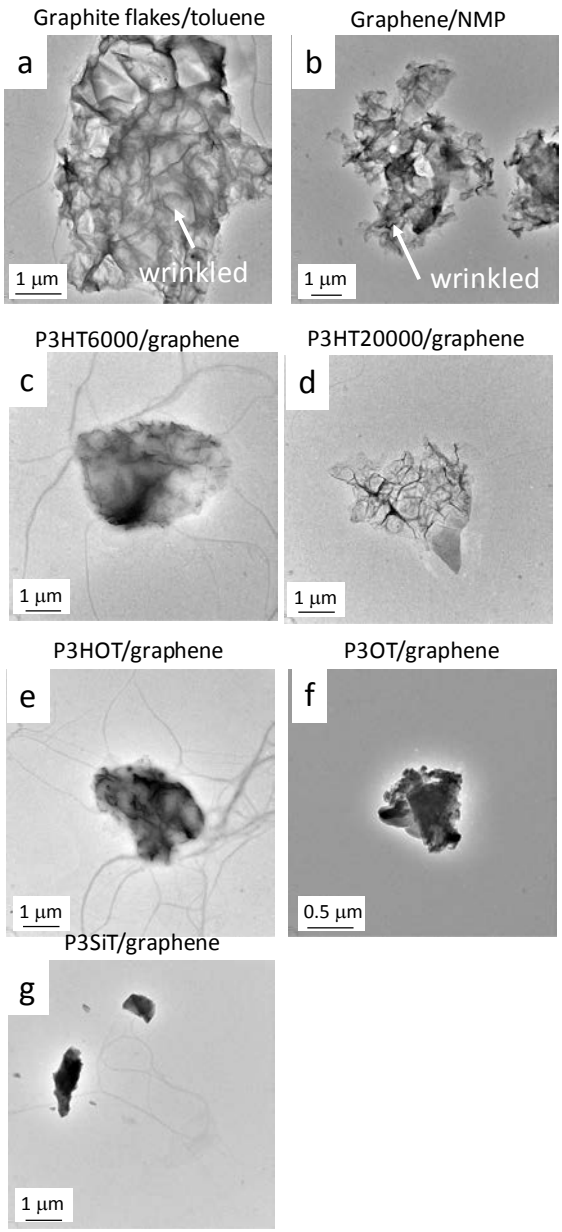

Fig. 6. TEM images of graphite flakes and PT/graphene complexes. (a) Graphite flakes in toluene, (b) multilayered graphene prepared in NMP, (c) P3HT6000/graphene complex, (d) P3HT20000/graphene complex, (e) P3HOT/graphene complex, (f) P3OT/graphene complex, and (g) P3SiT/graphene complex.

Transmission electron microscopy (TEM) and atomic force microscopy (AFM) were used to characterize the exfoliated multilayered graphene in detail. Fig. 6a and b show TEM images of graphite flakes dispersed in toluene and multilayered graphene prepared in NMP, respectively. These both exhibited wrinkled surfaces. Multilayered graphene prepared with P3HT6000 and P3HT20000 (Fig.

6c and d, respectively) were less wrinkled than the above graphite flakes and multilayered graphene in NMP, probably because the adsorption of P3HT kept the multilayered graphene extended. In the cases of P3HOT, P3OT and P3SiT, the multilayered graphene were insufficiently exfoliated (Fig. 6e, f and g, respectively), which was consistent with results from UV-Vis absorption measurements.

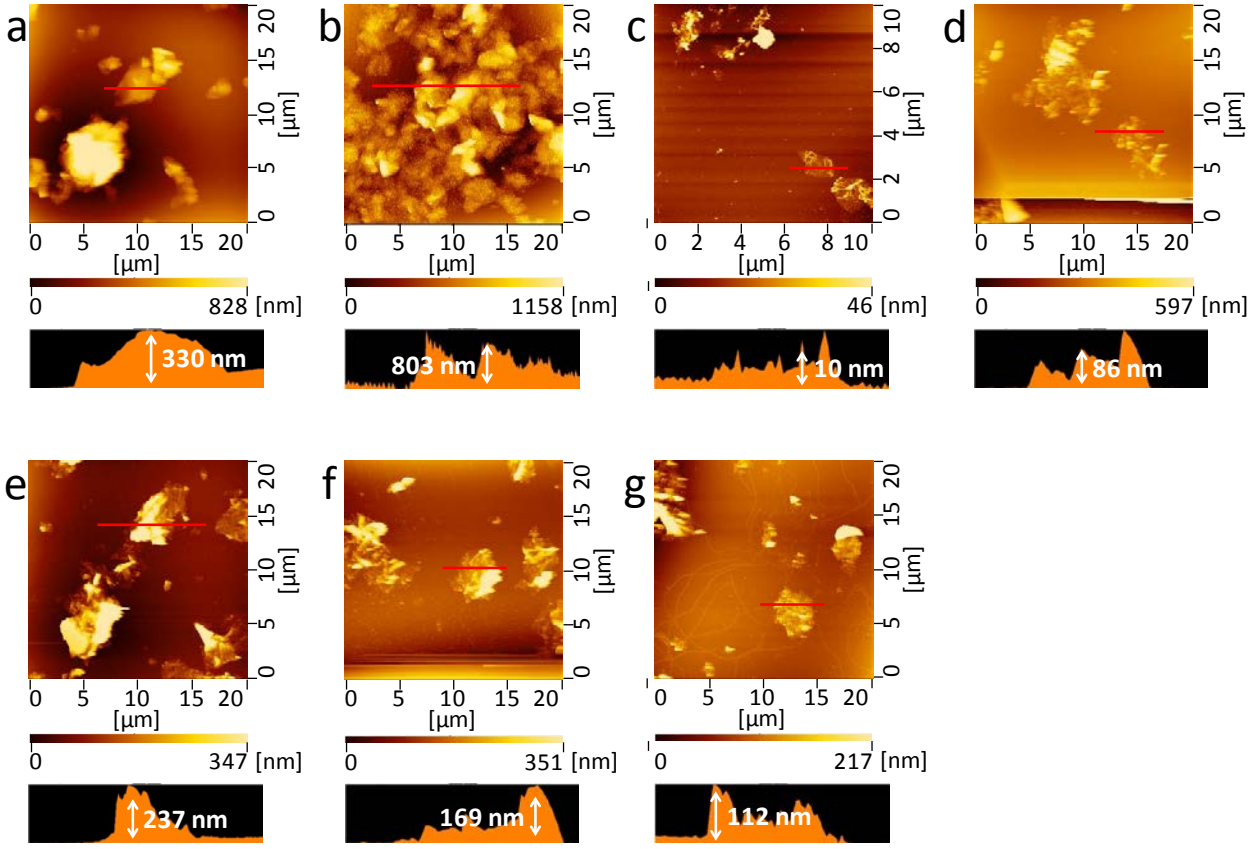

Fig. 7. AFM images of graphite flakes and washee PT/graphene complexes on silicon substrates with height profiles taken along the black lines. (a) Graphite flakes in toluene, (b) multilayered graphene in NMP, (c) P3HT6000/graphene complex, (d) P3HT20000/graphene complex, (e) P3HOT/graphene complex, (f) P3OT/graphene complex, and (g) P3SiT/graphene complex. Each lower panel represents a height profile at a red arrow of an upper panel.

AFM images also provided information on the morphology of the multilayered graphene (Fig. 7). A graphite flake dispersed in toluene and then dried on a silicon substrate was found to be 330 nm

thick, indicating that it was unexfoliated (Fig. 7a). Multilayered graphene prepared in NMP was found to be >800 nm thick. The height profile in Fig. 7b was uneven. A P3HT6000/graphene complex washed were thinner than approximately 10 nm and relatively flat (Fig. 7c), indicating multilayered graphene with P3HT6000. These results suggested that washing to remove excess P3HT6000 did not induce aggregation in the P3HT6000/graphene complex. The P3HT20000/graphene, P3HOT/graphene and P3SiT/graphene complexes were 80–240 nm thick (Fig. 7d–g), indicating the incomplete exfoliation of graphite flakes.

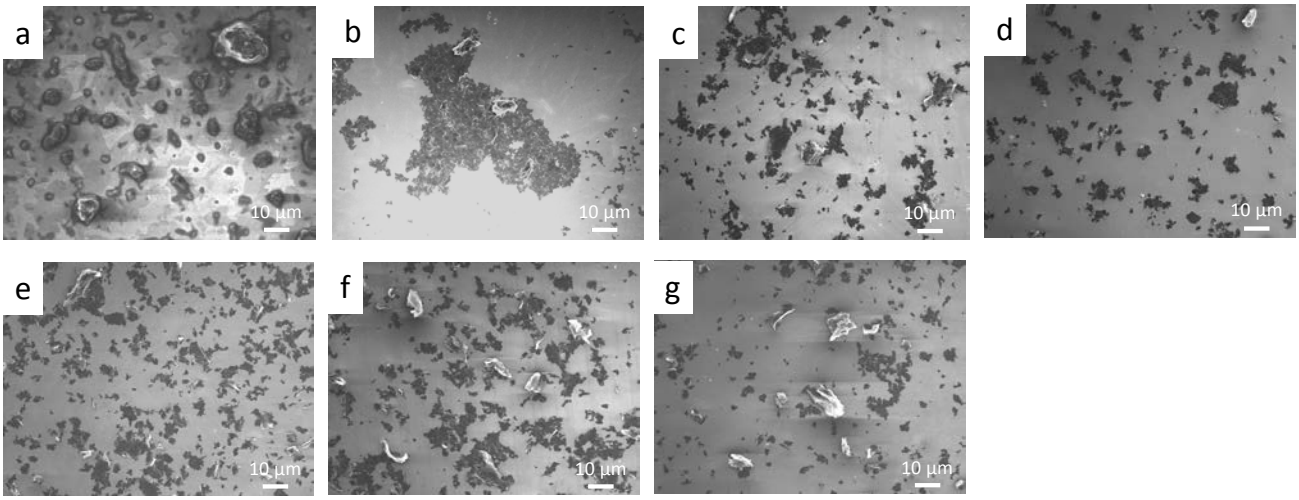

Fig. 8. FE-SEM images of graphite flakes and PT/graphene complexes. (a) Graphite flakes in toluene, (b) multilayered graphene prepared in NMP, (c) P3HT6000/graphene complex, (d) P3HT20000/graphene complex, (e) P3HOT/graphene complex, (f) P3OT/graphene complex, and (g) P3SiT/graphene complex.

FE-SEM observation can provide morphological information of many specimens of PT/graphene complexes at a time while TEM and AFM observation have limitation in the number of observable specimen. Fig. 8 shows the FE-SEM images of graphite flakes and PT/graphene complexes. Graphite flakes dispersed in toluene shows agglomerate more than 10 µm in diameter and with an obvious thickness, indicating unexfoliation of graphite. Multilayered graphene prepared in NMP seemed

aggregated and bulky in part. Many of P3HT6000/graphene and P3HT20000/graphene complexes were flat and non-aggregated although small portions of the complexes seemed bulky. P3HOT/graphene complexes were well-dispersed but bulky in part. Large portions of P3OT/graphene and P3SiT/graphene complexes were bulky, indicating insufficient exfoliation of graphite flakes. These results were consistent with those of AFM observations.

3.3. Electric resistance of PT/graphene complexes

To investigate the electrical property of the PT/graphene complexes, PT/graphene composites on filter paper were prepared by suction filtration of the graphene dispersion (Fig. S6). The sheet resistance of all the composites ranged from 28 to 57 Ωsq^{-1}. The P3OT/graphene composite resulted in the lowest resistance, meaning the highest conductivity. The sheet resistance of the P3HT6000/graphene composite was 32.8 ± 1.1 Ωsq^{-1}, which was slightly higher than that of the P3OT/graphene composite. These resistance values were much lower than that of our previous report (1.8 ± 0.5 $k\Omega sq^{-1}$) [44]. The major difference between the present and previous studies were the removal of extra PT from PT/graphene composites by washing with toluene, which might improve the electric conductivity of the composites. These investigations demonstrated that graphene complexes with PTs affords can be used as a conductive ink.

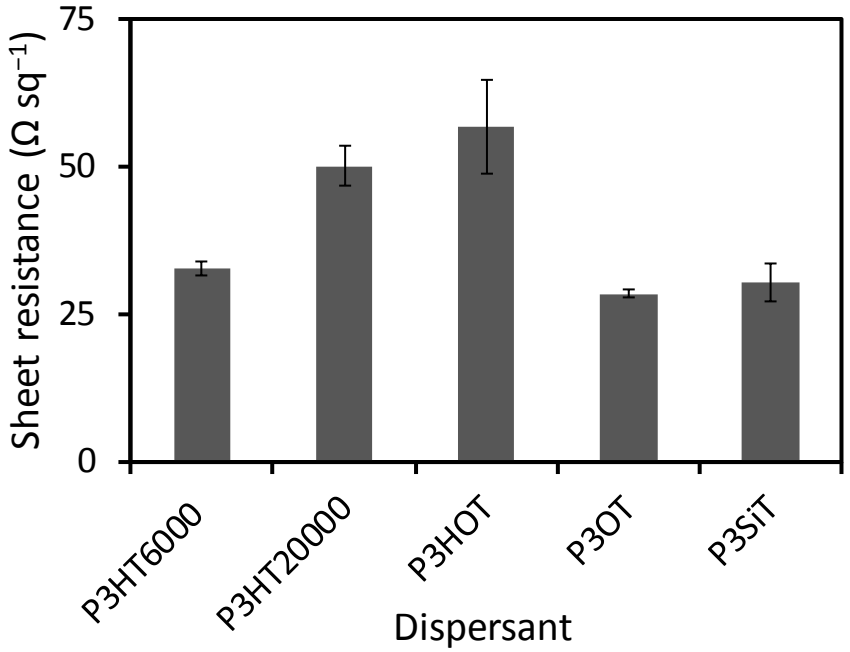

Fig. 9. Electric resistance of PT/graphene composites prepared on filter paper.

3.4. X-ray and thermogravimetric analyses of the P3HT/graphene complex.

Graphene frequently oxidizes during the exfoliation of graphite and the dispersion of graphene in solvents [55]. The oxidation resistances of multilayered graphene complexed with P3HT6000 were investigated by X-ray photoelectron spectroscopy. The P3HT/graphene complex had a sufficiently large carbon/oxygen ratio (C/O ratio = ~12, Fig. 10a) after ultrasonication for 5 h [23, 56], while the graphite flakes had a C/O ratio of 25. This indicated that the present exfoliation and washing procedures did not significantly oxidize the graphene, which accounted for the high electrical conductivity of the P3HT/graphene complex.

X-ray diffraction (XRD) was used to confirm that the multilayered graphene were not stacked, and to analyze the crystallization of P3HT6000. Fig. S7 shows XRD patterns of graphite flakes and the washed P3HT/graphene complex after drying. Graphite usually exhibits a sharp diffraction peak at 26° 2θ, which is the (002) diffraction of graphite and arises from the interlayer distance between

graphene sheets [57, 58]. The graphite flakes exhibited a weak broad diffraction at 20–30° 2θ [59]. The washed P3HT6000/graphene exhibited a similar weak broad diffraction at 20–30° 2θ, indicating no obvious stacking of graphene sheets. Pure P3HT6000 exhibits a diffraction peak at 5° 2θ, which arises from the edge-on crystallization of P3HT [49, 60]. This diffraction peak was not observed in the XRD pattern of the washed P3HT6000/graphene complex, indicating that no crystallization of P3HT6000 occurred within the complex.

Thermogravimetric analysis was carried out for the washed P3HT6000/graphene complex. Fig. 10b shows that the washed P3HT6000/graphene complex exhibited two major significant losses, which occurred at 160–350 °C and 350–800 °C. These were attributed to pyrolysis and gasification of P3HT6000 and the graphene, respectively. The mass percentages of P3HT and graphene were calculated to be 48% and 52%, respectively. This result was slightly inconsistent with that from the elemental analysis. The strong interaction of P3HT with the graphene may have affected the pyrolysis and gasification of the P3HT and graphene.

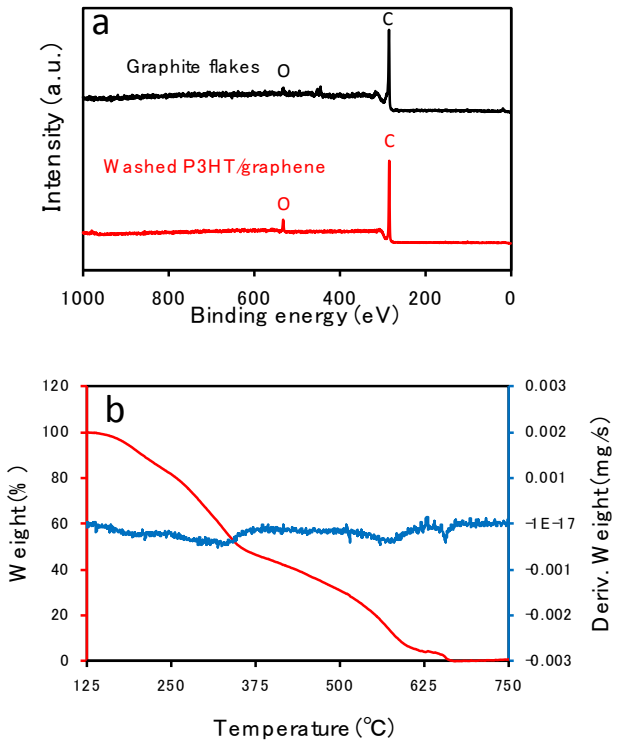

Fig. 10. (a) XPS spectra of graphite flakes (black) and washed P3HT6000/graphene complex (red). (b) Thermogravimetric (red) and first derivative thermogravimetric (blue) curves of the washed P3HT6000/graphene complex.

4. Conclusion

We have investigated the effects of the preparation conditions of polythiophene/graphene complexes on their dispersion in organic solvents, and on the in-solution morphology of the multilayered graphene. Among the tested PTs, P3HT with its low molecular weight most effectively exfoliated the graphite flakes and dispersed the ultrathin multilayered graphene in toluene. This led to a high yield for the P3HT/graphene complex. Spectroscopy analysis revealed the strong interaction between P3HT and the multilayered graphene. FPIA analysis provided information on the in-solution morphology of the PT/graphene complex before drying. Microscopy observations demonstrated that P3HT immobilized the extended morphology of the multilayered graphene during drying and that pristine multilayered graphene not containing P3HT shrunk during drying. All the tested PTs afforded highly conductive PT/graphene complexes. These findings further our understanding of the morphology of graphene, and will promote the development of wrinkleless graphene nanosheets.

Acknowledgments

The authors thank Prof. Nishino (Kobe Univ), Prof. Nishiyama (Kobe Univ), Prof. Taniya (Kobe Univ) and Prof. Nishina (Okayama Univ) for technical assistance with AFM observations, thermogravimetric analyses and FE-SEM observations. This research was supported partially by The Murata Science Foundation, Asahi Glass Foundation, Special Coordination Funds for Promoting Science and Technology, Creation of Innovation Centers for Advanced Interdisciplinary Research Areas (Innovative Bioproduction Kobe), MEXT, Japan, and by JSPS KAKENHI (Grant No. 16H04577).

Supplementary data

The following is the supplementary data related to this article:

Characterization of PTs synthesized, elemental analysis of PT/graphene complexes, UV-vis absorption spectra, FPIA analysis, optical microscope observation and X-ray diffraction analysis (PDF). Video of microscope observations of the multilayered graphene while drying. Movie S1 to S3.

Notes

The authors declare no competing financial interest.

References

[1] K.S. Novoselov, A.K. Geim, S.V. Morozov, D. Jiang, Y. Zhang, S.V. Dubonos, I.V. Grigorieva, A.A. Firsov, Electric field effect in atomically thin carbon films, Science 306(5696) (2004) 666-669.

[2] A.K. Geim, K.S. Novoselov, The rise of graphene, Nat. Mater. 6(3) (2007) 183-191.

[3] K.S. Novoselov, V.I. Fal'ko, L. Colombo, P.R. Gellert, M.G. Schwab, K. Kim, A roadmap for graphene, Nature 490(7419) (2012) 192-200.

[4] A. Reina, X. Jia, J. Ho, D. Nezich, H. Son, V. Bulovic, M.S. Dresselhaus, J. Kong, Large area, few-layer graphene films on arbitrary substrates by chemical vapor deposition, Nano Lett. 9(1) (2009) 30-35.

[5] K.S. Kim, Y. Zhao, H. Jang, S.Y. Lee, J.M. Kim, K.S. Kim, J.H. Ahn, P. Kim, J.Y. Choi, B.H. Hong, Large-scale pattern growth of graphene films for stretchable transparent electrodes, Nature 457(7230) (2009) 706-710.

[6] C. Berger, Z. Song, X. Li, X. Wu, N. Brown, C. Naud, D. Mayou, T. Li, J. Hass, A.N. Marchenkov, E.H. Conrad, P.N. First, W.A. de Heer, Electronic confinement and coherence in patterned epitaxial graphene, Science 312(5777) (2006) 1191-1196.

[7] A. Bianco, H.M. Cheng, T. Enoki, Y. Gogotsi, R.H. Hurt, N. Koratkar, T. Kyotani, M. Monthioux, C.R. Park, J.M.D. Tascon, J. Zhang, All in the graphene family - A recommended nomenclature for two-dimensional carbon materials, Carbon 65 (2013) 1-6.

[8] R.V. Salvatierra, C.E. Cava, L.S. Roman, M.M. Oliveira, A.J.G. Zarbin, The total chemical synthesis of polymer/graphene nanocomposite films, Chem. Commun. 52(8) (2016) 1629-1632.

[9] G. Cravotto, P. Cintas, Sonication-assisted fabrication and post-synthetic modifications of graphene-like materials, Chem. Eur. J. 16(18) (2010) 5246-5259.

[10] F. Torrisi, T. Hasan, W.P. Wu, Z.P. Sun, A. Lombardo, T.S. Kulmala, G.W. Hsieh, S.J. Jung, F. Bonaccorso, P.J. Paul, D.P. Chu, A.C. Ferrari, Inkjet-printed graphene electronics, ACS Nano 6(4) (2012) 2992-3006.

[11] J.N. Coleman, Liquid Exfoliation of Defect-Free Graphene, Acc. Chem. Res. 46(1) (2013) 14-22.

[12] A. Schlierf, P. Samori, V. Palermo, Graphene-organic composites for electronics: optical and electronic interactions in vacuum, liquids and thin solid films, J. Mater. Chem. C 2(17) (2014) 3129-3143.

[13] A. Ciesielski, P. Samori, Graphene via sonication assisted liquid-phase exfoliation, Chem. Soc. Rev. 43(1) (2014) 381-398.

[14] S. Haar, A. Ciesielski, J. Clough, H.F. Yang, R. Mazzaro, F. Richard, S. Conti, N. Merstorf, M. Cecchini, V. Morandi, C. Casiraghi, P. Samori, A supramolecular Strategy to Leverage the Liquid-Phase Exfoliation of Graphene in the Presence of Surfactants: unraveling the role of the length of fatty acids, Small 11(14) (2015) 1691-1702.

[15] P. Wick, A.E. Louw-Gaume, M. Kucki, H.F. Krug, K. Kostarelos, B. Fadeel, K.A. Dawson, A. Salvati, E. Vazquez, L. Ballerini, M. Tretiach, F. Benfenati, E. Flahaut, L. Gauthier, M. Prato, A. Bianco, Classification framework for graphene-based materials, Angew. Chem. Int. Ed. 53(30) (2014) 7714-7718.

[16] Y. Hernandez, V. Nicolosi, M. Lotya, F.M. Blighe, Z.Y. Sun, S. De, I.T. McGovern, B. Holland,

M. Byrne, Y.K. Gun'ko, J.J. Boland, P. Niraj, G. Duesberg, S. Krishnamurthy, R. Goodhue, J. Hutchison, V. Scardaci, A.C. Ferrari, J.N. Coleman, High-yield production of graphene by liquid-phase exfoliation of graphite, Nat. Nanotechnol. 3(9) (2008) 563-568.

[17] P. Laaksonen, M. Kainlauri, T. Laaksonen, A. Shchepetov, H. Jiang, J. Ahopelto, M.B. Linder, Interfacial engineering by proteins: exfoliation and functionalization of graphene by hydrophobins, Angew. Chem. Int. Ed. 49(29) (2010) 4946-4949.

[18] Y.T. Liang, M.C. Hersam, Highly concentrated graphene solutions via polymer enhanced solvent exfoliation and iterative solvent exchange, J. Am. Chem. Soc. 132(50) (2010) 17661-17663.

[19] L. Guardia, M.J. Fernandez-Merino, J.I. Paredes, P. Solis-Fernandez, S. Villar-Rodil, A. Martinez-Alonso, J.M.D. Tascon, High-throughput production of pristine graphene in an aqueous dispersion assisted by non-ionic surfactants, Carbon 49(5) (2011) 1653-1662.

[20] J.N. Coleman, M. Lotya, A. O'Neill, S.D. Bergin, P.J. King, U. Khan, K. Young, A. Gaucher, S. De, R.J. Smith, I.V. Shvets, S.K. Arora, G. Stanton, H.Y. Kim, K. Lee, G.T. Kim, G.S. Duesberg, T. Hallam, J.J. Boland, J.J. Wang, J.F. Donegan, J.C. Grunlan, G. Moriarty, A. Shmeliov, R.J. Nicholls, J.M. Perkins, E.M. Grieveson, K. Theuwissen, D.W. McComb, P.D. Nellist, V. Nicolosi, Two-dimensional nanosheets produced by liquid exfoliation of layered materials, Science 331(6017) (2011) 568-571.

[21] A.S. Wajid, S. Das, F. Irin, H.S.T. Ahmed, J.L. Shelburne, D. Parviz, R.J. Fullerton, A.F. Jankowski, R.C. Hedden, M.J. Green, Polymer-stabilized graphene dispersions at high concentrations in organic solvents for composite production, Carbon 50(2) (2012) 526-534.

[22] P. He, C. Zhou, S.Y. Tian, J. Sun, S.W. Yang, G.Q. Ding, X.M. Xie, M.H. Jiang, Urea-assisted aqueous exfoliation of graphite for obtaining high-quality graphene, Chem. Commun. 51(22) (2015) 4651-4654.

[23] M. Matsumoto, Y. Saito, C. Park, T. Fukushima, T. Aida, Ultrahigh-throughput exfoliation of graphite into pristine 'single-layer' graphene using microwaves and molecularly engineered ionic

liquids, Nat. Chem. 7(9) (2015) 730-736.

[24] V. Georgakilas, A. Demeslis, E. Ntararas, A. Kouloumpis, K. Dimos, D. Gournis, M. Kocman, M. Otyepka, R. Zboril, Hydrophilic nanotube supported graphene–water dispersible carbon superstructure with excellent conductivity, Adv. Funct. Mater. 25(10) (2015) 1481-1487.

[25] A. Ciesielski, P. Samori, Supramolecular approaches to graphene: from self-assembly to molecule-assisted liquid-phase exfoliation, Adv. Mater. 28(29) (2016) 6030-6051.

[26] V. Georgakilas, M. Otyepka, A.B. Bourlinos, V. Chandra, N. Kim, K.C. Kemp, P. Hobza, R. Zboril, K.S. Kim, Functionalization of graphene: covalent and non-covalent approaches, derivatives and applications, Chem. Rev. 112(11) (2012) 6156-214.

[27] S.K. Deng, V. Berry, Wrinkled, rippled and crumpled graphene: an overview of formation mechanism, electronic properties, and applications, Mater. Today 19(4) (2016) 197-212.

[28] Y.H. Zhang, H.R. Zhang, B. Wang, Z.Y. Chen, Y.Q. Zhang, B. Wang, Y.P. Sui, B. Zhu, C.M. Tang, X.L. Li, X.M. Xie, G.H. Yu, Z. Jin, X.Y. Liu, Role of wrinkles in the corrosion of graphene domain-coated Cu surfaces, Appl. Phys. Lett. 104(14) (2014) 143110.

[29] A. Isacsson, L.M. Jonsson, J.M. Kinaret, M. Jonson, Electronic superlattices in corrugated graphene, Phys. Rev. B 77(3) (2008) 035423.

[30] C.H. Lui, L. Liu, K.F. Mak, G.W. Flynn, T.F. Heinz, Ultraflat graphene, Nature 462(7271) (2009) 339-41.

[31] C.G. Wang, Y.P. Liu, L. Lan, H.F. Tan, Graphene wrinkling: formation, evolution and collapse, Nanoscale 5(10) (2013) 4454-4461.

[32] J.H. Mun, B.J. Cho, Synthesis of monolayer graphene having a negligible amount of wrinkles by stress relaxation, Nano Lett. 13(6) (2013) 2496-2499.

[33] X. Shen, X.Y. Lin, N. Yousefi, J.J. Jia, J.K. Kim, Wrinkling in graphene sheets and graphene oxide papers, Carbon 66 (2014) 84-92.

[34] W.J. Chen, X.C. Gui, B.H. Liang, M. Liu, Z.Q. Lin, Y. Zhu, Z.K. Tang, Controllable fabrication

of large-area wrinkled graphene on a solution surface, ACS Appl. Mater. Interfaces. 8(17) (2016) 10977-10984.

[35] R.D. McCullough, The chemistry of conducting polythiophenes, Adv. Mater. 10(2) (1998) 93-116.

[36] D. Tasis, N. Tagmatarchis, A. Bianco, M. Prato, Chemistry of carbon nanotubes, Chem. Rev. 106(3) (2006) 1105-36.

[37] B.K. Kuila, S. Malik, S.K. Batabyal, A.K. Nandi, In-situ synthesis of soluble poly(3-hexylthiophene)/multiwalled carbon nanotube composite: Morphology, structure, and conductivity, Macromolecules 40(2) (2007) 278-287.

[38] V. Saini, Z.R. Li, S. Bourdo, E. Dervishi, Y. Xu, X.D. Ma, V.P. Kunets, G.J. Salamo, T. Viswanathan, A.R. Biris, D. Saini, A.S. Biris, Electrical, optical, and morphological properties of P3HT-MWNT nanocomposites prepared by in situ polymerization, J. Phys. Chem. C 113(19) (2009) 8023-8029.

[39] A. Chunder, J.H. Liu, L. Zhai, Reduced graphene oxide/poly(3-hexylthiophene) supramolecular composites, Macromol. Rapid. Commun. 31(4) (2010) 380-384.

[40] Z.L. Yang, X.J. Shi, J.J. Yuan, H.T. Pu, Y.S. Liu, Preparation of poly(3-hexylthiophene)/graphene nanocomposite via in situ reduction of modified graphite oxide sheets, Appl. Surf. Sci. 257(1) (2010) 138-142.

[41] R. Bkakri, N. Chehata, A. Ltaief, O.E. Kusmartseva, F.V. Kusmartsev, M. Song, A. Bouazizi, Effects of the graphene content on the conversion efficiency of P3HT: Graphene based organic solar cells, J. Phys. Chem. Solids 85 (2015) 206-211.

[42] K. Zhang, L.L. Zhang, X.S. Zhao, J.S. Wu, Graphene/polyaniline nanofiber composites as supercapacitor electrodes, Chem. Mater. 22(4) (2010) 1392-1401.

[43] K. Chi, Z.Y. Zhang, J.B. Xi, Y.A. Huang, F. Xiao, S. Wang, Y.Q. Liu, Freestanding graphene paper supported three-dimensional porous graphene-polyaniline nanocomposite synthesized by inkjet printing and in flexible all-solid-state supercapacitor, ACS Appl. Mater. Interfaces. 6(18) (2014)

16312-16319.

[44] H. Iguchi, C. Higashi, Y. Funasaki, K. Fujita, A. Mori, A. Nakasuga, T. Maruyama, Rational and practical exfoliation of graphite using well-defined poly(3-hexylthiophene) for the preparation of conductive polymer/graphene composite, Sci. Rep. 7 (2017) 39937.

[45] H.W. Lee, Y. Yoon, S. Park, J.H. Oh, S. Hong, L.S. Liyanage, H.L. Wang, S. Morishita, N. Patil, Y.J. Park, J.J. Park, A. Spakowitz, G. Galli, F. Gygi, P.H.S. Wong, J.B.H. Tok, J.M. Kim, Z.A. Bao, Selective dispersion of high purity semiconducting single-walled carbon nanotubes with regioregular poly(3-alkylthiophene)s, Nat. Commun. 2 (2011) 541.

[46] S. Tamba, S. Tanaka, Y. Okubo, H. Meguro, S. Okamoto, A. Mori, Nickel-catalyzed dehydrobrominative polycondensation for the practical preparation of regioregular poly(3-substituted thiophene)s, Chem. Lett. 40(4) (2011) 398-399.

[47] S. Tamba, K. Shono, A. Sugie, A. Mori, C-H functionalization polycondensation of chlorothiophenes in the presence of nickel catalyst with stoichiometric or catalytically generated magnesium amide, J. Am. Chem. Soc. 133(25) (2011) 9700-9703.

[48] A. Mori, K. Ida, S. Tamba, S. Tsuji, Y. Toyomori, T. Yasuda, Synthesis and properties of regioregular poly(3-substituted thiophene) bearing disiloxane moiety in the substituent. Remarkably high solubility in hexane, Chem. Lett. 43(5) (2014) 640-642.

[49] K. Fujita, Y. Sumino, K. Ide, S. Tamba, K. Shono, J. Shen, T. Nishino, A. Mori, T. Yasuda, Synthesis of poly(3-substituted-thiophene)s of remarkably high solubility in hydrocarbon via nickel-catalyzed deprotonative cross-coupling polycondensation, Macromolecules 49(4) (2016) 1259-1269.

[50] V.G. Kravets, A.N. Grigorenko, R.R. Nair, P. Blake, S. Anissimova, K.S. Novoselov, A.K. Geim, Spectroscopic ellipsometry of graphene and an exciton-shifted van Hove peak in absorption, Phys. Rev. B 81(15) (2010) 155413.

[51] Z.P. Sun, T. Hasan, F. Torrisi, D. Popa, G. Privitera, F.Q. Wang, F. Bonaccorso, D.M. Basko, A.C. Ferrari, Graphene mode-locked ultrafast laser, ACS Nano 4(2) (2010) 803-810.

[52] F. Bonaccorso, Z. Sun, T. Hasan, A.C. Ferrari, Graphene photonics and optoelectronics, Nat. Photonics 4(9) (2010) 611-622.

[53] D.L. Meng, S.J. Yang, D.M. Sun, Y. Zeng, J.H. Sun, Y. Li, S.K. Yan, Y. Huang, C.W. Bielawski, J.X. Geng, A dual-fluorescent composite of graphene oxide and poly(3-hexylthiophene) enables the ratiometric detection of amines, Chem. Sci. 5(8) (2014) 3130-3134.

[54] T. Komabayashi, L.S.W. Spangberg, Comparative analysis of the particle size and shape of commercially available mineral trioxide aggregates and Portland cement: A study with a flow particle image analyzer, J. Endod. 34(1) (2008) 94-98.

[55] U. Khan, A. O'Neill, M. Lotya, S. De, J.N. Coleman, High-concentration solvent exfoliation of graphene., Small 6(7) (2010) 864-871.

[56] S. Yang, S. Bruller, Z.S. Wu, Z.Y. Liu, K. Parvez, R.H. Dong, F. Richard, P. Samori, X.L. Feng, K. Mullen, Organic radical-assisted electrochemical exfoliation for the scalable production of high-quality graphene, J. Am. Chem. Soc. 137(43) (2015) 13927-13932.

[57] Y.L. Hsin, K.C. Hwang, C.T. Yeh, Poly(vinylpyrrolidone)-modified graphite carbon nanofibers as promising supports for PtRu catalysts in direct methanol fuel cells, J. Am. Chem. Soc. 129(32) (2007) 9999-10010.

[58] K.S. Subrahmanyam, S.R.C. Vivekchand, A. Govindaraj, C.N.R. Rao, A study of graphenes prepared by different methods: characterization, properties and solubilization, J. Mater. Chem. 18(13) (2008) 1517-1523.

[59] C. Higashi, Y. Funasaki, H. Iguchi, T. Maruyama, In situ polymerization of a novel surfactant on a graphene surface for the stable dispersion of graphene in water, RSC Adv. 6(91) (2016) 88244-88247.

[60] T. Matsumoto, K. Nishi, S. Tamba, M. Kotera, C. Hongo, A. Mori, T. Nishino, Molecular weight effect on surface and bulk structure of poly(3-hexylthiophene) thin films, Polymer 119 (2017) 76-82.

Supplementary data

Preparation of uncurled and planar multilayered graphene using polythiophene derivatives via liquid-phase exfoliation of graphite

Hiroki Iguchi,[1] Koki Miyahara,[1] Chisato Higashi,[1] Keisuke Fujita,[1] Naoki Nakagawa,[1] Shunsuke Tamba,[1] Atsunori Mori,[1] Hiroshi Yoshitani,[2] Akira Nakasuga,[2] and Tatsuo Maruyama[1,*]

[1]Department of Chemical Science and Engineering, Graduate School of Engineering, Kobe University, 1-1 Rokkodaicho, Nada-ku, Kobe 657-8501, Japan

[2]Sekisui Chemical Co., Ltd., 2-1 Hyakuyama, Shimamoto-cho, Mishima-gun, Osaka 618-0021, Japan

Table S1. Molecular weights and regioregularities of the synthesized polythiophene derivatives.

Entry	M_n[a]	M_w/M_n[a]	Regioregularity %*
P3HT6000	5500	1.07	97
P3HT20000	18200	1.13	99
P3OT	23100	1.29	99
P3HOT	17000	1.31	99
P3SiT	21100	1.19	99

[a]M_n and M_w values were measured by GPC.[1, 2]

[b]The regioregularity was determined from NMR measurements.[2, 3]

Table S2. Elemental analysis of PT/graphene complexes and compositions of PTs in the dry complexes

Sample	S (%)	PT (wt%)
P3HT6000/graphene	3.60	19
P3HT20000/graphene	3.97	21
P3HOT/graphene	3.75	23
P3OT/graphene	4.59	28
P3SiT/graphene	2.36	21

The elemental analysis was carried out by Techno Science (Moriyama, Japan).

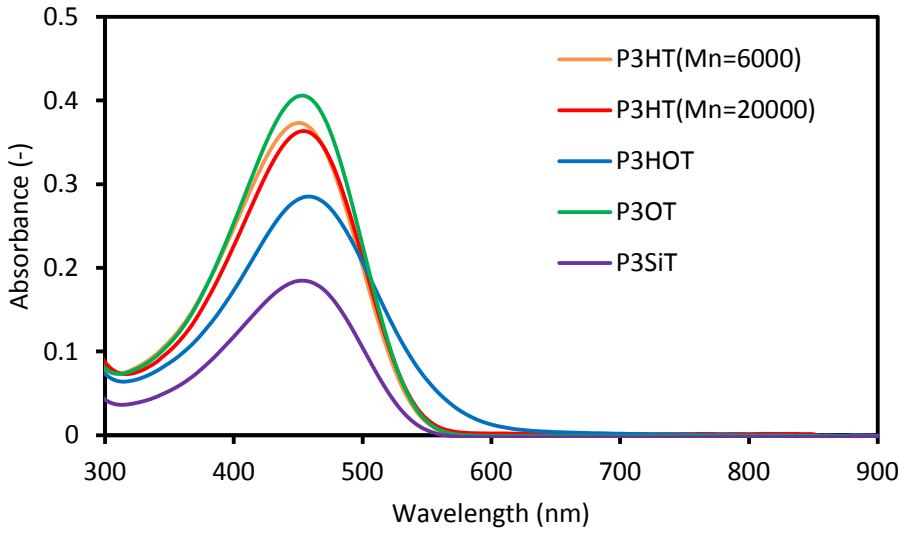

Fig. S1. Absorption spectra of PT solutions in toluene. The PT concentrations were 1.0 µg/ml.

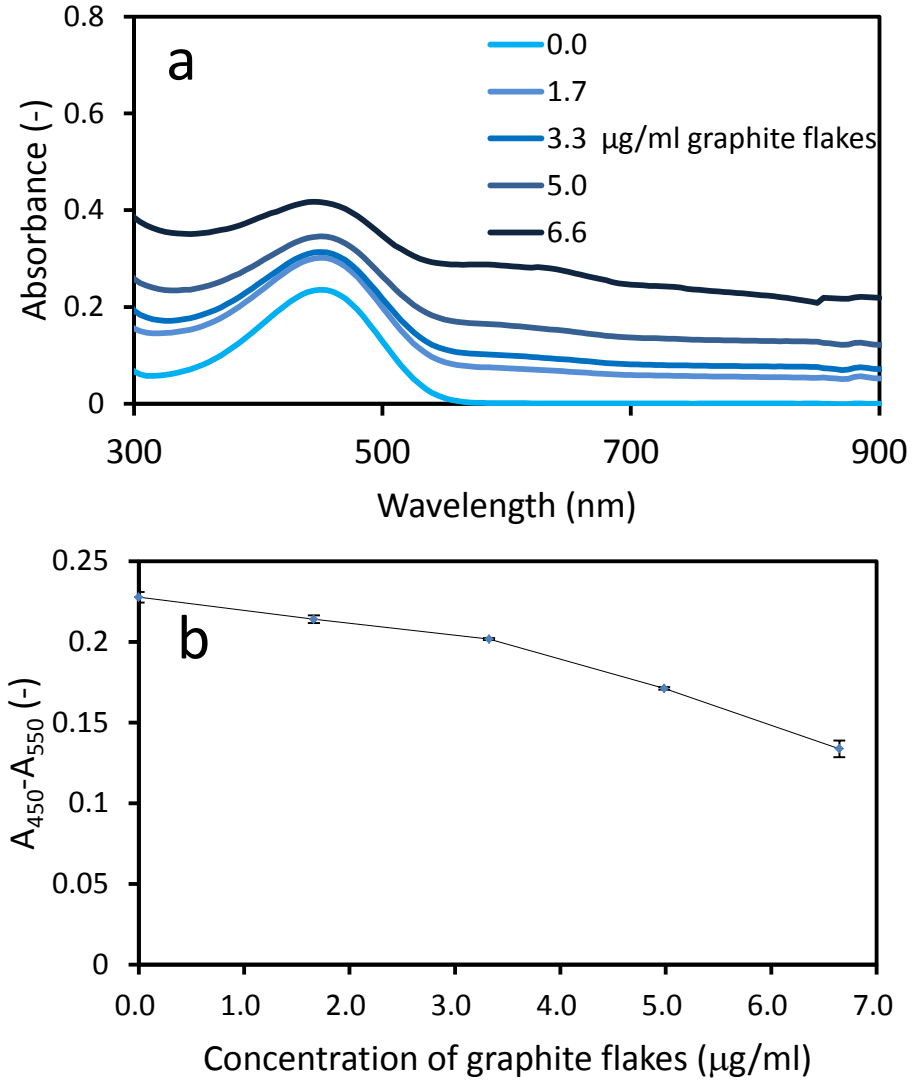

Fig. S2. (a) Effect of graphite flake concentration on absorption spectra of P3HT6000/graphene dispersions. (b) Effect of graphite flake concentration on the relative absorbance at 450 nm (Abs_{450}–Abs_{550}). The concentration of P3HT6000 was 6.6 µg/ml. The concentrations of the graphite flakes were 0, 1.7, 3.3, 5.0, and 6.6 µg/ml.

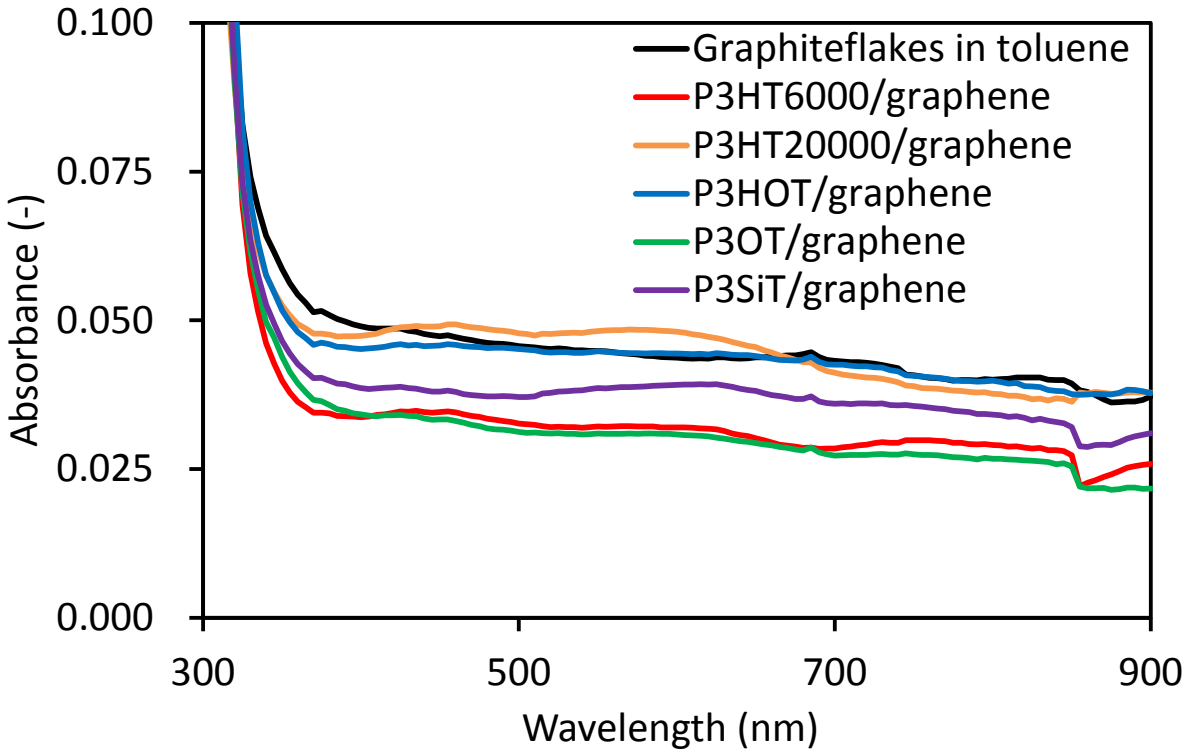

Fig. S3. UV-Vis absorption spectra of graphite flakes and PT/graphene dispersions in toluene. PT/graphene complexes were washed prior to measurement to remove excess PT.

a)

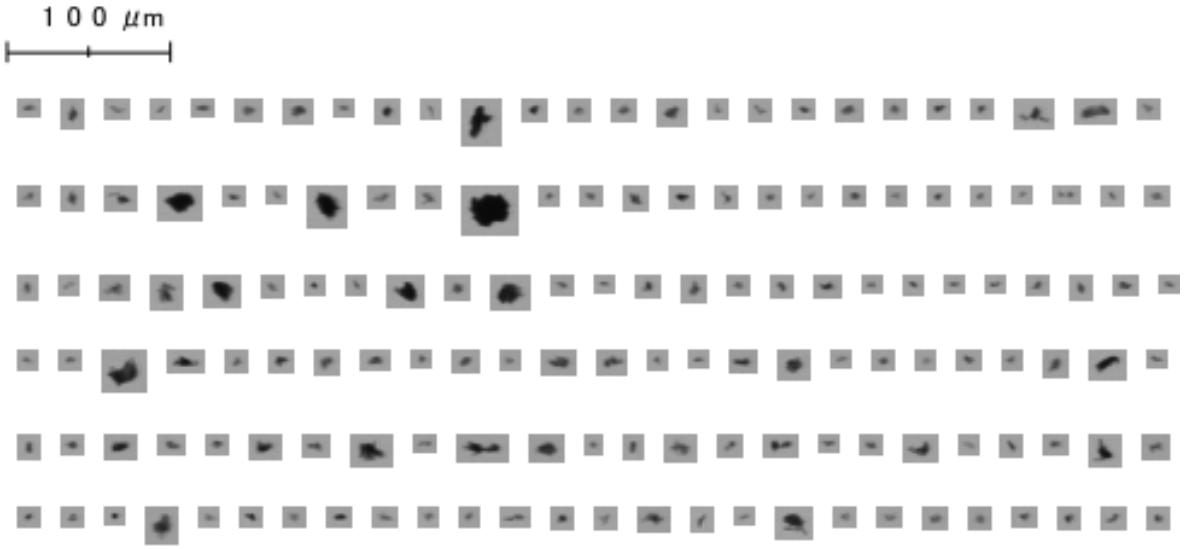

b)

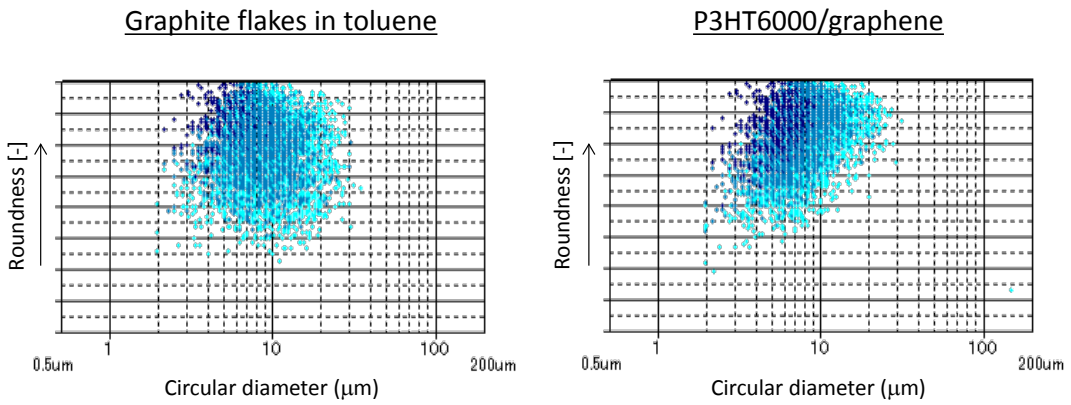

Number of particles : 12245
Equivalent circle diameter: 6.44 μm
Roundness: 0.85

Number of particles: 28832
Equivalent circle diameter : 4.85 μm
Roundness: 0.89

Fig. S4. (a) Representative particle images of the P3HT6000/graphene complex in toluene, as obtained by FPIA. (b) Scatter plots of graphite flakes in toluene and P3HT6000/graphene dispersion in toluene. The color strength indicates the particle frequency, with darker colors indicating more particles.

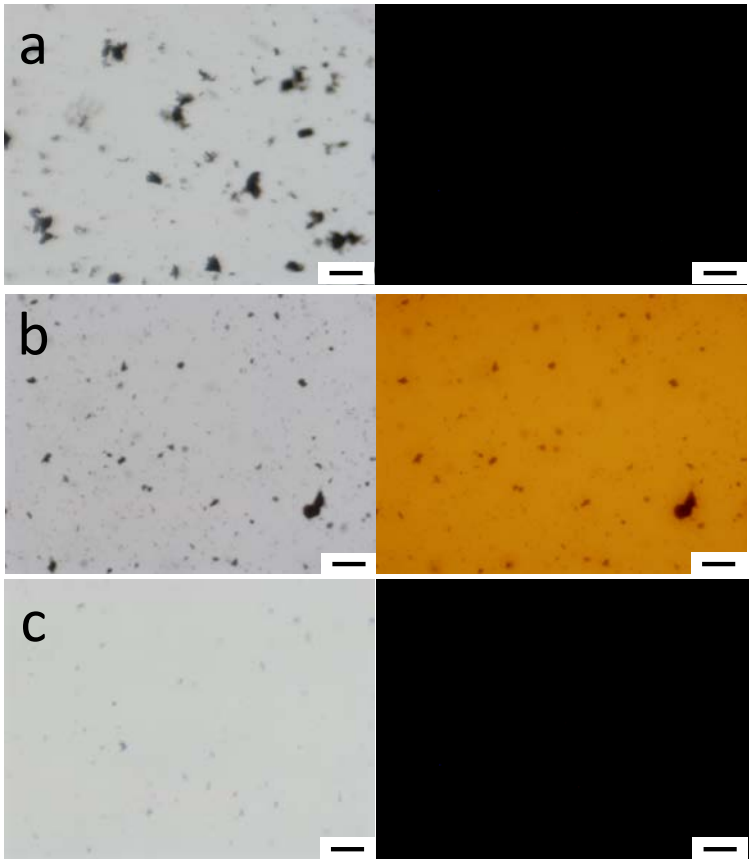

Fig. S5. Optical microscopy images of (a) graphite flakes in toluene, (b) P3HT6000/graphene dispersion before washing, and (c) P3HT6000/graphene dispersion after washing. The left column shows bright-field microscopy images and the right column shows fluorescence microscopy images. The observations were carried out under wet conditions. Scale bars represent 20 μm.

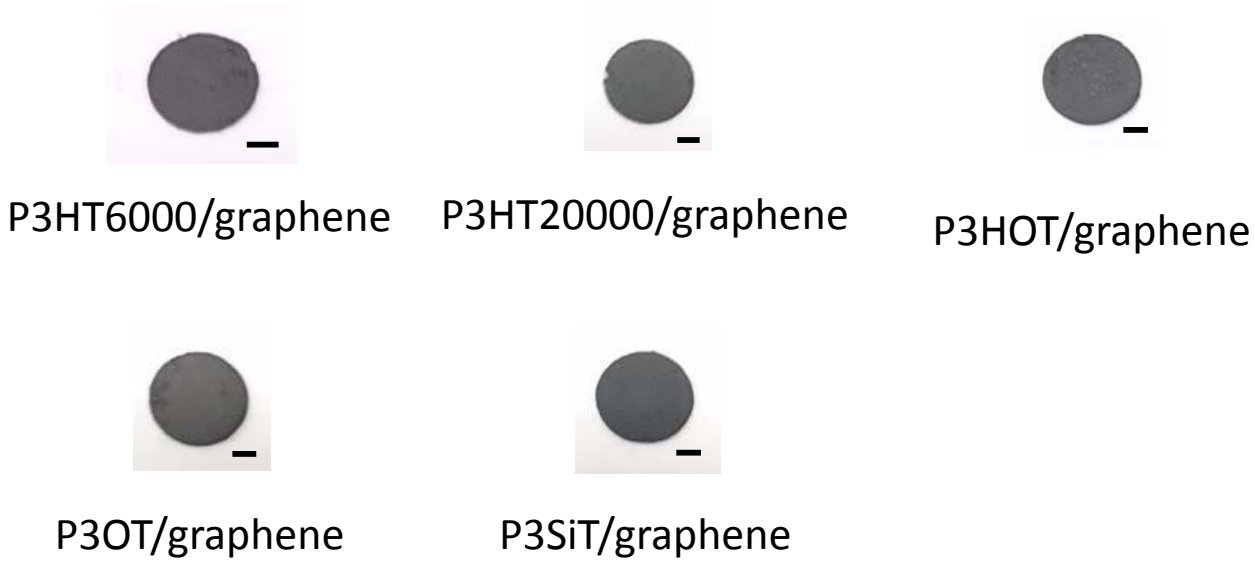

Fig. S6. Photos of PT/graphene composites prepared on filter paper. Scale bars represent 2.0 nm.

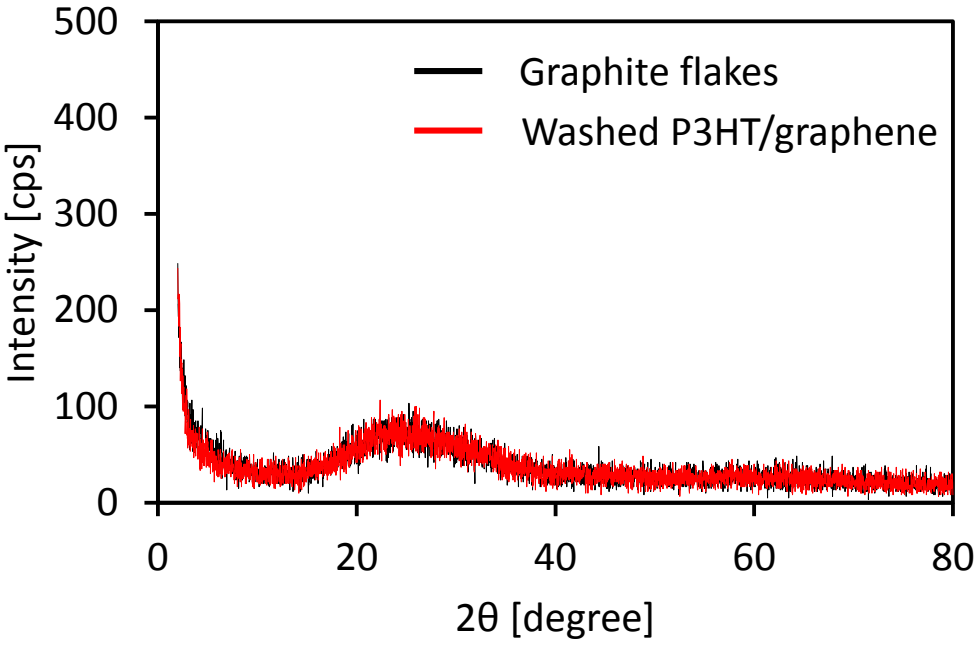

Fig. S7. XRD patterns of graphite flakes and the washed P3HT6000/graphene complex.

REFERENCES

1. Fujita, K.; Sumino, Y.; Ide, K.; Tamba, S.; Shono, K.; Shen, J.; Nishino, T.; Mori, A.; Yasuda, T., Synthesis of Poly(3-substituted thiophene)s of Remarkably High Solubility in Hydrocarbon via Nickel-Catalyzed Deprotonative Cross-Coupling Polycondensation. *Macromolecules* **2016,** 49, (4), 1259-1269.

2. Tamba, S.; Tanaka, S.; Okubo, Y.; Meguro, H.; Okamoto, S.; Mori, A., Nickel-catalyzed Dehydrobrominative Polycondensation for the Practical Preparation of Regioregular Poly(3-substituted thiophene)s. *Chem. Lett.* **2011,** 40, (4), 398-399.

3. Mori, A.; Ida, K.; Tamba, S.; Tsuji, S.; Toyomori, Y.; Yasuda, T., Synthesis and Properties of Regioregular Poly(3-substituted thiophene) Bearing Disiloxane Moiety in the Substituent. Remarkably High Solubility in Hexane. *Chem. Lett.* **2014,** 43, (5), 640-642.

Supplementary Movie S1 to S3

http://www.lib.kobe-u.ac.jp/repository/90005135.files/90005135_supple.html